Journal of the European Ceramic Society 22 (2002) 423–434

www.elsevier.com/locate/jeurceramsoc

Deposition of meso-porous γ-alumina coatings on ceramic honeycombs by sol-gel methods

Christos Agrafiotis[a,*], Athena Tsetsekou[b]

[a]*Department of Materials Science and Engineering, University of Ioannina, University Campus, 45110, Ioannina, Greece*
[b]*Department of Mineral Resources Engineering, Technical University of Crete, University Campus, 73100 Chania, Greece*

Received 11 January 2001; received in revised form 10 April 2001; accepted 21 April 2001

Abstract

The deposition of meso-porous γ-alumina coatings on multi-channeled cordierite honeycombs via sol–gel methods was investigated with the aim to correlate the deposition characteristics such as loading percentage, thickness and integrity of the coating to the support pore structure properties. Even though the mean pore size of the honeycomb supports was much higher than the size of the deposited particles, proper adjustment of sol viscosity prevented penetration of the sol into the support and led to the formation of a smooth coating of uniform, adjustable thickness. Sol viscosity was adjusted with the addition of poly-vinyl-alcohol (PVA) and with sol concentration by controlled evaporation, and fine-tuned in order to control loading percentage from 2 to 8 wt.% per impregnation, corresponding to coating thickness from 2 to approximately 10 μm respectively. The mean pore diameter of the support was found to affect the loading percentage. However, scanning electron microscopy observations have revealed that a very high loading percentage almost inevitably induces cracks on the coatings surface. The combination of sols and slurries of powders as coating media seems to be the optimum technical solution that can provide for satisfactory loading percentage per impregnation together with structural integrity of the coating.

Keywords: Catalyst supports; Coatings; Cordierite; γ-Al_2O_3; Membranes; Sol-gel methods

1. Introduction

The combination of high gas flow rates and elevated temperatures encountered in applications such as automotive catalysis, catalytic combustion and hot gas cleanup, have established ceramic thin-wall multi-channeled honeycombs (monoliths) as the structural substrate of choice.[1–3] Honeycombs can accommodate high gas flow rates with small pressure drop, whereas high temperatures can be tolerated with the use of cordierite ($2MgO*2Al_2O_3*5SiO_2$), a ceramic material with relatively high melting point and excellent thermal shock resistance (or of other materials with similar properties). Since cordierite honeycombs possess an inherently low surface area, the catalytically active component is present on the monolith walls supported on a finely divided, high-surface area material (called carrier or secondary support so that it is not confused with the "primary" support, the honeycomb). Among the various choices for carrier materials, γ-alumina is the most commonly used, since (with the addition of rare earth compounds) it can maintain a high surface area within a wide temperature range (600–1000°C). The carrier is usually applied by the impregnation of the honeycomb in a slurry of finely ground alumina powder (dip-coating or washcoating).[1,2]

High-surface area γ-alumina can be prepared via sol-gel methods from liquid organic or inorganic precursor materials.[4] Sol-gel routes have the inherent advantages of extremely active products with high surface area, controllable and facile incorporation of other compounds such as promoters or stabilizers, fine-tuning of the products' pore structure and direct casting of the alumina layer on the support. Impregnation of the honeycombs can be done directly with a sol and upon drying and calcination, a well-adhered coating layer can be formed in situ upon the support walls. In this respect, the preparation of alumina-based catalyst supports via sol-gel methods has many common characteristics with the preparation and deposition of supported alumina membranes.[5–8] Especially relevant are studies concerned with the thermal stability of either materials[9,10] since

* Corresponding author. Tel.: +30-6519-7398; fax: +30-6519-7034.
E-mail address: chagrafi@cc.uoi.gr (C. Agrafiotis).

0955-2219/02/$ - see front matter
PII: S0955-2219(01)00295-3

these studies involve addition of the same kind of rare earth compounds, and monitoring of the membrane/catalyst carrier properties such as pore structure, phase transformations and surface area after thermal treatment.

As with the case of membrane synthesis, the major obstacles in preparing catalyst carrier coatings directly from sols lie in the post-synthesis stages such as layer deposition, drying and sintering, where the sol properties have to be matched with the pore structure of the particular supports. A "technical" advantage in the preparation of catalyst carriers compared to that of membranes is that in the former, the coating integrity is not such a crucial requirement : pinholes and even micro-cracks that can significantly alter the permeation characteristics of a membrane, can be tolerated in a catalytic carrier as long as they do not lead to spalling from the support.

Membranes are usually very thin and because of their fragility, are often supported on sintered robust ceramic supports that have a mean pore size of 1–2 μm, of flat or tubular geometry (discs, hollow tubes) depending on the particular application.[5–10] The situation is far more complicated in the case of catalytic carriers for high temperature applications that have to be deposited upon ceramic honeycombs. First of all, in order to provide a high total surface area, the carrier layer should be relatively thick (10–100 μm; however, the inherent high surface area of sol-gel prepared carriers can reduce the thickness required). The complex honeycomb geometry imposes further problems with respect to coating uniformity which has to be achieved both along the length of a channel as well as across the monolith cross-section area from channel to channel. Finally, cordierite honeycombs, in order to perform satisfactorily under the high temperature gradients encountered in such applications, have to exhibit specific values of both porosity and mean pore diameter. These can be fine-tuned by proper adjustment of the sintering cycle during their manufacture,[11] but usually the mean pore diameter is adjusted in the range of 3–30 μm and their porosity between 30 and 45%.[1–3] Low-viscosity sols because of their very fine particle size, can very easily penetrate into the porous structure of such a support, rather than form a surface coating easily accessible to the gaseous reactants.[12] Thus, the complex geometry of the support combined with the significant mismatch between the pore size of the honeycomb and the size of the sol particles, render the deposition of thick, smooth, surface coatings on honeycombs by sol-gel methods, a real challenge.

Correlation of the deposition characteristics (sol viscosity, particle size etc.) to the support properties (porosity, pore size distribution) is thus necessary, in order to tailor the deposition of coatings with specific characteristics (thickness, pore size, permeability etc.) upon specific supports. However, only a limited number of studies deals with correlation of the microstructure of the porous support to the properties of the coating layer formed.[13–15] Deposition of γ-alumina membranes upon asymmetric tubular supports of graded porosity[13,14] has shown that sol viscosity is one of the most crucial factors in determining the membrane quality as well as the loading. High-viscosity sols form films that develop cracks during drying and calcination, which of course affect adversely the membrane separation ability. Cracks could be avoided if sufficiently thin films (<10 μm) were prepared. In another study, dealing with the deposition of SnO_2 membranes, the effect of the properties of two different supports, alumina and kaolin was compared.[15] Even though the two supports had similar pore diameter ($d_{p50}\cong 0.67$ μm), the quality of the membranes deposited upon alumina was much better, a fact that was attributed, by the authors, to the narrower pore structure of alumina compared to that of kaolin.

Usually, γ-alumina membranes are prepared from sols obtained by the peptization of boehmite suspensions in water with nitric acid.[7] The synthesis of supported and unsupported γ-alumina membranes is described in a series of publications by Burggraaf and co-workers.[15–21] They have developed membranes on porous supports with thickness up to 20 μm and pore sizes in the range 25–40 Å. The membrane thickness was found to depend on the dipping time and on the support pore size.[16] However, very thick membranes had a tendency to crack because of the residual stresses developed during drying, thus an optimum thickness (around 5 μm) was determined for the formation of crack-free membranes. The use of additives such as poly-vinyl-alcohol (PVA) was found on one hand to adjust the sol viscosity[17] and on the other hand to control the drying rate, helping to decrease significantly the number of cracks.[18] However, in all of the studies above, the supports were α-alumina discs with very low mean pore diameter (0.2 μm). The use of PVA has been also employed by other researchers for the production of crack-free, thermally stable (with lanthania doping) multi-layered γ-alumina membranes.[22–24]

In this work, the deposition of thin γ-alumina coatings via sol-gel routes upon cordierite honeycomb specimens was studied. The aim was to deposit smooth, homogeneous, strongly adhered coatings upon cordierite honeycomb substrates of given pore size distribution, as well as to correlate the deposition characteristics (coating thickness, loading percentage) to the support properties such as porosity and pore size distribution. The parameters investigated were mainly the sol viscosity and the pore size of the support.

2. Experimental

Cylindrical cordierite specimens manufactured by Ceramics and Refractories Technological Development

Company (CERECO) Greece, with 400 square cells/in^2 (typical dimensions: diameter 1.5 cm and length 2 cm) were used as supports. In such honeycombs each channel has a square cross-section with dimensions 1×1 mm, whereas the wall thickness is 200 μm. Details of manufacturing as well as of the tuning of the porosity and of the pore size distribution have been reported elsewhere.[11]

The γ-alumina layer deposition was carried out by dip-coating from the liquid phase using a sol prepared with a dispersible commercial colloidal pseudo-boehmite (γ-AlOOH) powder.[a] This powder, upon calcination in the temperature range 500–700°C converts to the γ-alumina phase. The solids content of the sol was kept constant at 10 wt.%, because beyond this value the sol viscosity increased significantly and the sol was not suitable for homogeneous coating. The sol pH was adjusted to 4.0 by the addition of HNO_3. The sol viscosity was adjusted by the addition of two different, highly viscous PVA-based binders (denoted hereafter Binder 1,[b] and Binder 2[c]) — a technique very common in membrane preparation.[23–25] Further adjustment of sol viscosity took place with sol concentration by evaporation at 70°C under vacuum. In all cases the sol viscosity was measured with the aid of a rotating-spindle viscometer (Brookfield RVT DV-II). Sets of measurements with a specific spindle were taken at all rotational speeds where a reading of the viscosity value could be obtained.

The cordierite specimens were immersed in the sols for 1 min. Three to five samples were examined per case, in order to check for the reproducibility of results. The loaded specimens were withdrawn, the sol remaining in the channels was allowed to drain, and removal of excess sol that formed menisci on the channel walls was achieved by blowing air through the honeycomb channels. Subsequently the coated honeycombs were dried at 110°C for 2 h and calcined at 600°C for 2 h, so that a γ-alumina coating adhering to the substrate could be formed. The loading percentage was determined by the increase of specimen weight after calcination. Mercury (Quantachrome Autoscan A33 porosimeter) as well as nitrogen (Micromeritics ASAP 2000 porosimeter) porosimetry was used for the determination of the pore size distribution of the uncoated and the coated honeycombs. The morphology of the coated specimens and the quality of the deposited layers (cracking, adhesion on the support) were studied with the aid of scanning electron microscopy (Jeol-6300 microscope). An overview of the course of the experiments, the parameters varied and a quantitative description of the results obtained are summarized in Table 1.

[a] Disperal, Condea GmbH, Germany.

[b] Erkol 23/88, (aqueous solution 12 wt.%), Rhodia, Tarragona, Spain.

[c] Optapix PAF 3, Zschimmer & Schwarz Gmbh & Co, Lahnstein, Germany.

3. Results — discussion

In this work, in order to study the correlation between support pore structure and sol rheological properties, two batches of honeycombs were prepared, with the same porosity (30%), but with different mean pore diameters (d_{p50}) of 10 and 3 μm (denoted hereafter Support 1 and Support 2 respectively). It should be again stressed here that these pore diameters are significantly higher than respective support pore diameters reported in many studies on the preparation of supported γ-alumina membranes.[16–21]

When impregnation of the honeycombs took place with the initial sol (10 wt.% commercial boehmite powder, no binder addition, no concentration), the low sol viscosity, favored the penetration of the sol into the pores of the cordierite support, rather than the formation of a surface coating layer. The morphology of a monolith coated with such a sol is shown in Fig. 1a and can be compared with that of a monolith coated with a slurry of γ-alumina powder shown in Fig. 1b. Because of the high water content in the gel, large shrinkage takes place during drying and calcination, which induces extensive cracking. Cracked gel blocks can be very clearly seen in the pores of the support. Smaller pores are completely filled with the gelled sol and blocked, whereas larger pores are partially filled or remain empty. After impregnation with this particular sol, the absence of a continuous surface layer is clear: practically the whole amount of the deposited powder is distributed throughout the pore structure of the support, in contrast to the monolith coated with powder slurry, where a coating about 5 μm thick has formed upon the exterior surface of the honeycomb wall. This phenomenon is frequently observed in the literature, when the rheological properties of the sol are not fine-tuned to match the pore structure of the given support.[12] Apart from fine-tuning the sol viscosity, another solution frequently employed, is the deposition of an intermediate layer with smaller mean pore diameter than that of the original support and the creation of a multi-layered structure with gradually decreasing pore size.[18,23,24]

In order to increase the sol viscosity, two PVA-based binders with different viscosity were employed. The viscosity of the two binders as a function of the rotational speed of the viscometer spindle (which is proportional to the shear rate applied) is shown in Fig. 2. Binder 2 behaves as a Newtonian fluid, exhibiting an almost constant viscosity value around 7000 mPa s^{-1} in the whole range of shear rates studied, whereas Binder 1 exhibits a pseudoplastic behavior, its viscosity decreasing with increasing shear rate. The viscosity of Binder 2 is three to four times higher than that of Binder 1. For further adjustment of the sol viscosity, and in addition to the use of binder, the sols were concentrated (water evaporation) by heating at 70°C under vacuum. The upper limit of sol concentration

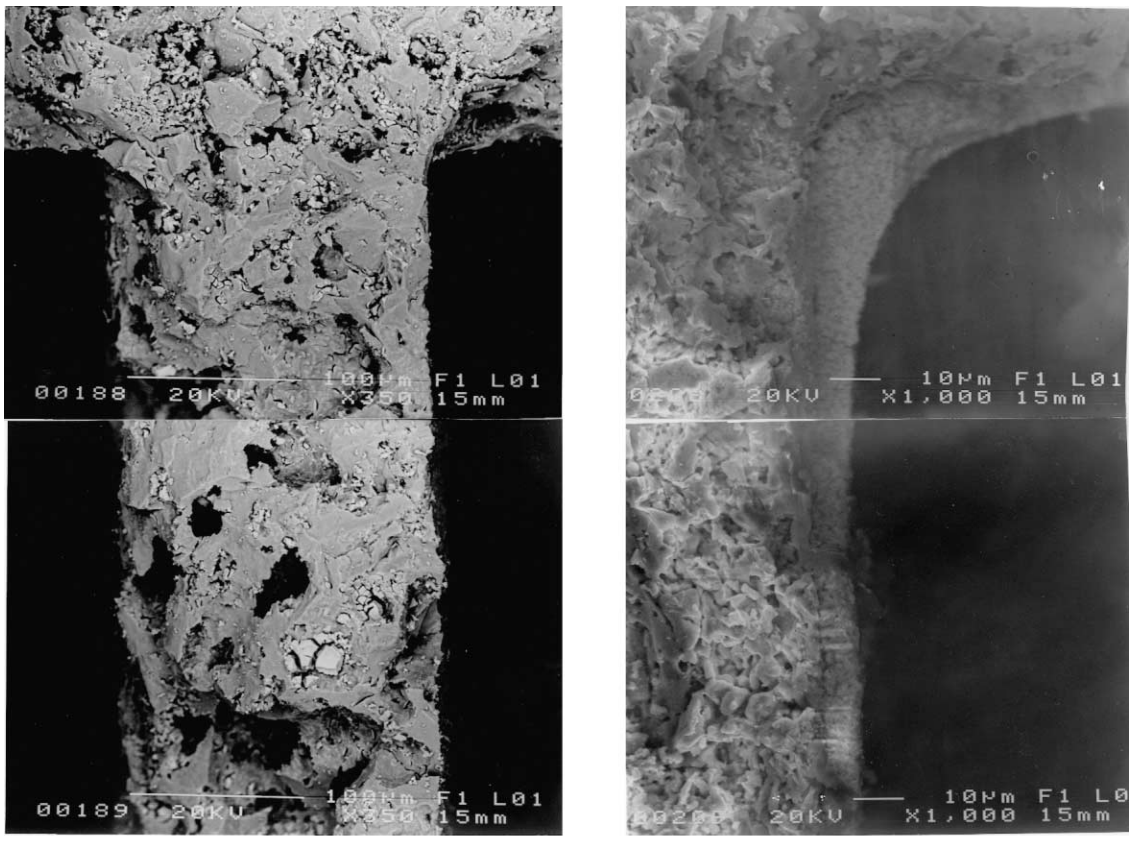

(a) (b)

Fig. 1. (a) Coating with a boehmite sol. Effect of sol viscosity on coating process: penetration and gelation of the sol in the pores of the substrate, due to low viscosity (support: $d_{p50} = 10$ μm). (b) Coating of the same honeycomb with a powder slurry (particle characteristic diameter $d_{90} = 2$ μm).

Table 1
Outline of the course of the experiments performed, the parameters varied and the corresponding results

Experiments performed	Parameters varied	Results
Preparation of honeycombs with similar porosity but different mean pore diameter	Heating rate (see Ref. 11)	•Supports with porosity ≈30% and $d_{p50} = 10$ μm and $d_{p50} = 3$ μm
Adjustment of sol viscosity by binder addition and sol concentration	Binder addition (kind and percentage of binder)	•Slight increase of sol viscosity
		•Low loading percentage (⩽2 wt.%) •Sol penetration into the support pores
	Degree of sol concentration (0–60% of initial weight)	•Drastic increase of sol viscosity •"Parabolic-law" increase of loading percentage with increasing sol viscosity •High loading percentage (up to 8 wt.%) •Loading percentage depends on support pore diameter for high-viscosity sols •Surface (no penetration), meso-porous coating ($d_{p50} = 7.0$ nm) •Coating integrity deteriorates with increasing loading percentage
Use of sol/powder slurry mixed systems	Sol/powder proportion	•No binder addition needed •Higher loading percentage (12.5–13.5 wt.%) •Maintenance of coating integrity at high loadings •Surface coating (no penetration), excellent adhesion

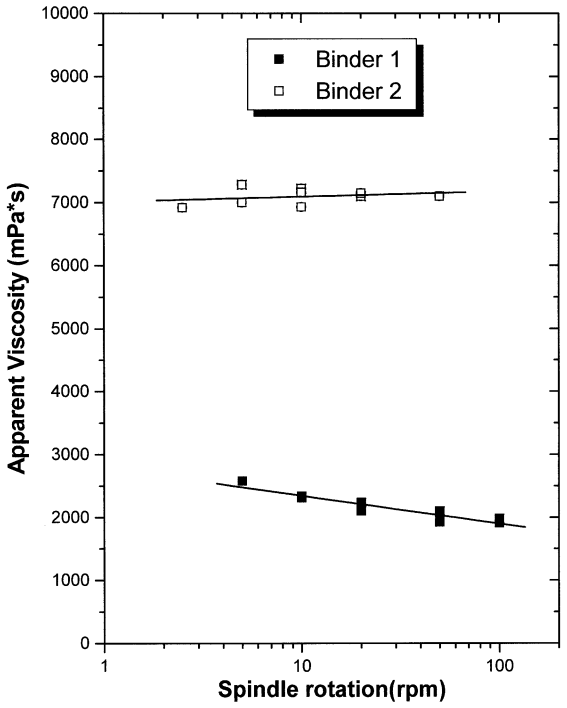

Fig. 2. Viscosity of the two binders employed, as a function of shear rate.

was about 45 wt.% of the initial sol weight; beyond that point the sol viscosity increased significantly, producing a very viscous paste, which could not be homogenized and uniformily deposited.

The effect of binder addition and sol concentration on sol viscosity is shown in Table 2. It can be observed that, even in the case of the highly viscous binder, addition of binder alone up to 20 wt.%, does not increase significantly the sol viscosity. Sol concentration, following the binder addition, is required for a substantial increase of sol viscosity. Under these circumstances the effect of the binder viscosity becomes much more prominent: for the same percentage of sol concentration, sols with the highly viscous binder (No. 2) are much more viscous.

The effect of sol viscosity on the loading percentage achieved is summarized in Table 2 and depicted in Fig. 3. Loading percentage is expressed as the weight of coating material deposited after the calcination step, per initial weight of uncoated support. Results from all the coated specimens with a sol of a particular viscosity are shown, in order to observe the effect of sol viscosity on the reproducibility of the coating process. In all cases, the concentration step increased the sol viscosity (Table 2) and consequently the loading percentage (Fig. 3) from 0.5 to 8.2 wt.% (achieved with a single impregnation). However, as the sol becomes more viscous, on one hand loading percentage approaches a plateau value and on the other hand the scattering among the loading values achieved with the same sol, becomes larger. A very viscous sol tends to settle irregularly on the honeycomb walls and its excess removal with the stream of hot air is not always homogeneous and reproducible. As a result, discrepancies in loading among samples loaded with the same sol are more frequently observed.

The effect of the support pore size can be observed in Fig. 4 where the average loading percentage values obtained with the two batches of honeycombs are plotted as a function of sol viscosity. For each support, results obtained with both binders are plotted together. For the two support pore size distributions examined ($d_{p50} = 3$ and 10 μm) there was no significant difference in loading percentage when the sol had low or intermediate viscosity (below 250 mPa s^{-1}). When the sol viscosity exceeded

Table 2
Effect of binder addition and sol concentration on sol viscosity and loading percentage achieved, for the two supports tested

Coating medium	Binder 1			Binder 2		
		Support mean pore size = 10 μm	Support mean pore size = 3 μm		Support mean pore size = 10 μm	Support mean pore size = 3 μm
	Viscosity (mPa s^{-1})	Loading percentage (wt.%)	Loading percentage (wt.%)	Viscosity (mPa s^{-1})	Loading percentage (wt.%)	Loading percentage (wt.%)
Boehmite sols: initial solids content (before concentration): 10 wt.%						
No binder–no sol concentration	15	1.55	1.60	15	1.55	1.60
10% Binder–no sol concentration	19.2	1.92	2.05	23.5	1.63	1.78
20% Binder–no sol concentration	27.5	1.86	1.87	41.4	2.00	1.95
20% Binder–sol concentration: with Binder 1: to 55% of initial weight with Binder 2: to 59% of initial weight	80.6	3.61	3.45	212	4.72	4.54
20% Binder–sol concentration: with Binder 1: to 40.7% of initial weight with Binder 2: to 42.8% of initial weight	1160	7.80	6.51	1700	8.21	7.18
Boehmite sol/slurry of $Al(OH)_3$ powder						
Solids content: 50 wt.% No binder–no sol concentration	63	12.5–13.5				

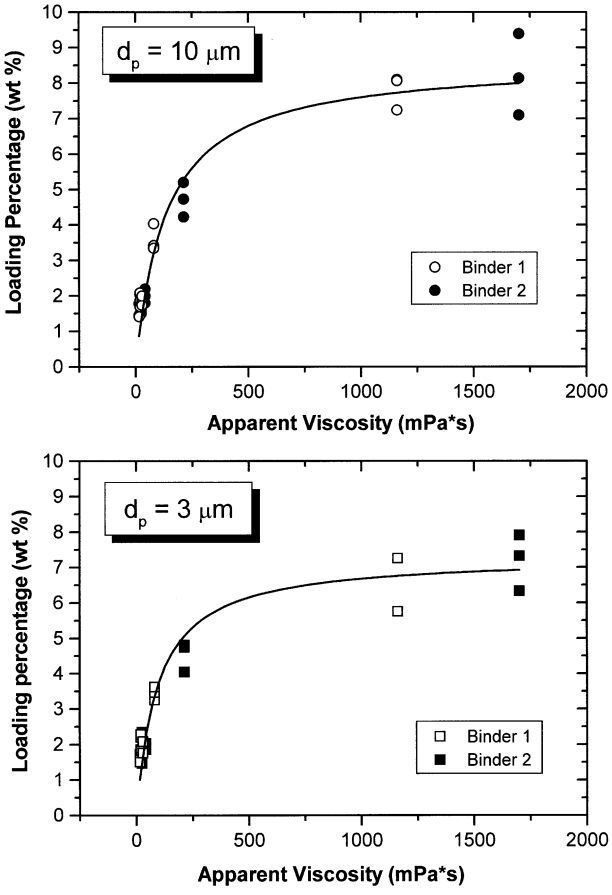

Fig. 3. Loading percentage and reproducibility achieved as a function of sol viscosity.

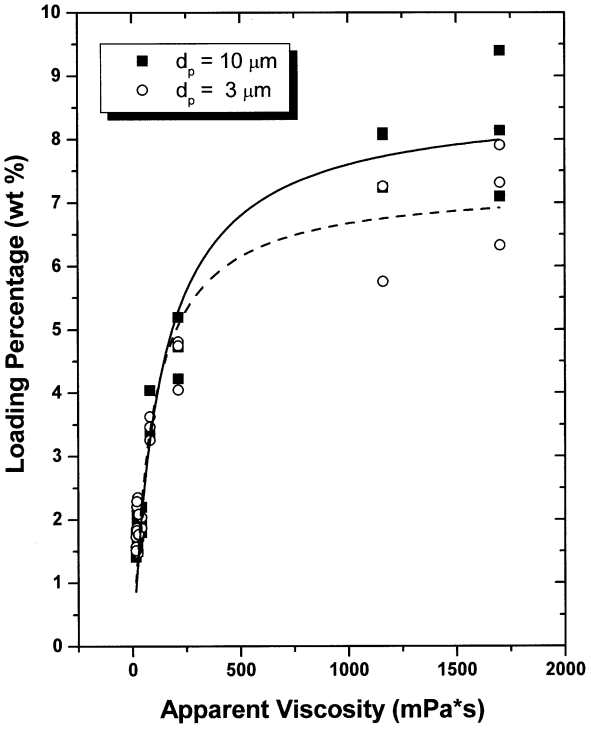

Fig. 4. Average values of loading percentage achieved as a function of sol viscosity, for the two substrates used.

this value, an increase of the loading percentage was observed for the support with the higher mean pore diameter, which reached ~8 wt.% at 1700 mPa s^{-1}, compared to 7 wt.% for the 3 μm support.

The dependence of the thickness of the deposited layer on the sol viscosity can be very clearly observed in

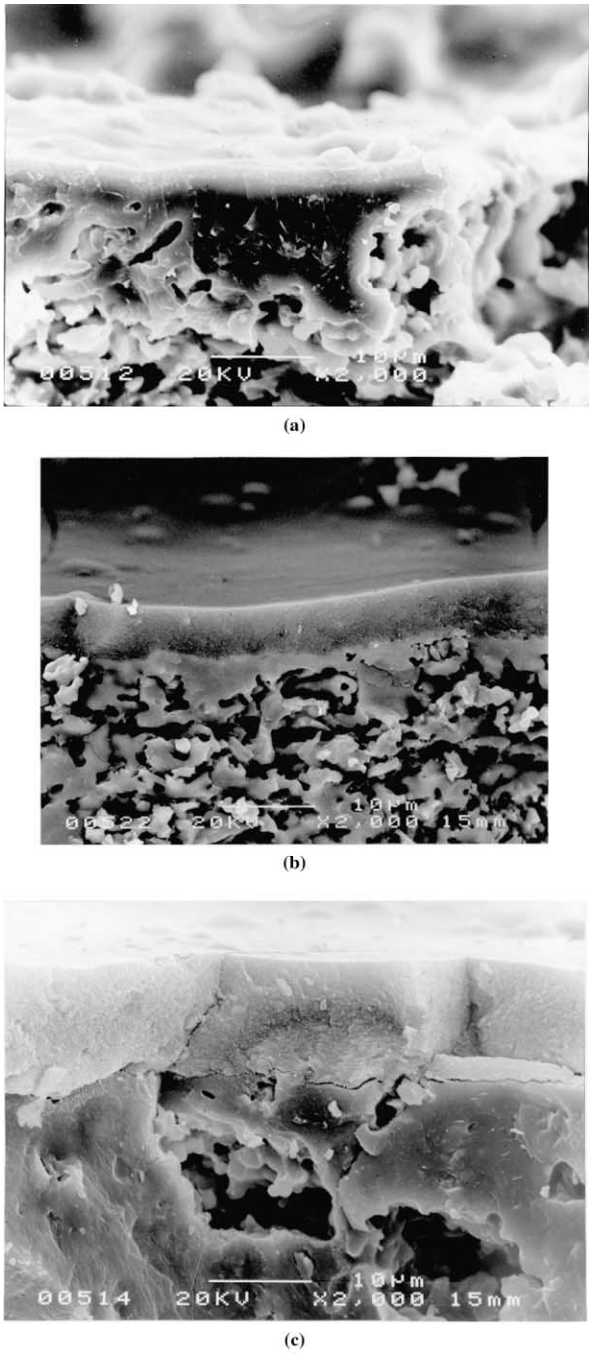

Fig. 5. Effect of sol viscosity on the thickness of the deposited coating. Scanning electron microscopy photographs (under the same magnification of 2000×) of the substrate-coating interface for a honeycomb with mean pore size $d_p = 10$ μm, coated with a sol containing 20 wt.% binder: (a) no sol concentration; (b) concentration of the sol to 55% of its initial weight; (c) concentration of the sol to 40 wt.% of its initial weight.

the sequence of photographs presented in Fig. 5 where the coating/substrate interface is depicted for the substrate with $d_{p50} = 10$ μm, for three different cases. In Fig. 5a the case of deposition from a sol with addition of 20 wt.% of Binder 1 and without any sol concentration is shown. The viscosity of this sol was 27.5 mPa s^{-1} and the loading percentage achieved was 1.86 wt.%. A smooth coating layer with a thickness in the range 1–2 μm is observed on the external channel surface. The washcoat/substrate interfaces in the cases of the sols with 20 wt.% of the same binder, which in addition had been concentrated to 55 and 40% of their initial weight (respective viscosities 80.6 and 1160 mPa s^{-1}), are compared in Figs. 5b and c under the same magnification. There is a gradual transition from a coating about 2 μm thick to one of about 7 μm and finally to one more than 10 μm thick (all achieved with a single impregnation). The coating thickness is a reflection of the higher loading percentage achieved (from 1.86, 3.61 and 7.8 wt.% respectively) as the sol viscosity is increased.

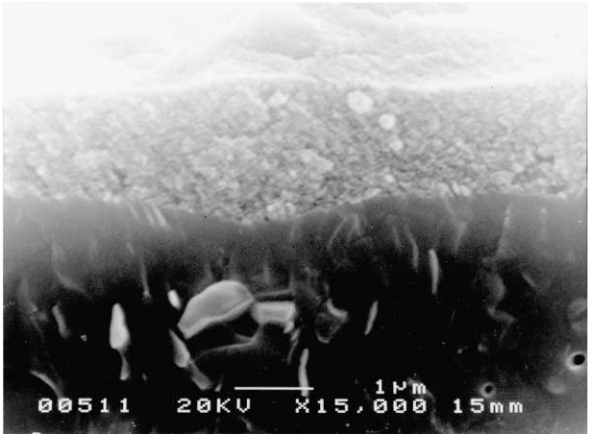

Fig. 6. Detail of Fig. 5a (deposition from a sol containing 20 wt.% binder without sol concentration) showing the coating/substrate interface.

A magnification of the coating/substrate interface shown in Fig. 5a. is presented in Fig. 6. The fine coating particles (much finer than the support mean pore diameter) have gelled on the channel surface and formed a closely packed layer on the macroporous support. A sharp and clear coating/substrate interface can be distinguished.

The difference in loading percentage observed at high viscosities between the two porous supports (Fig. 3), can be explained if we take a closer look at the mechanisms that take place during the coating of macro-porous supports (like the honeycombs used in this study) with a sol of colloidal particles. The formation of the coating layer on the support surface takes place by two mechanisms. The first contribution is from capillary suction. As the sol is brought into contact with the channel walls of the dry porous support, capillary forces drive the water through the support leaving behind a layer of concentrated sol on the support surface. A filtration process takes place, similar to that of the slip-casting process[17] and a "cake" of deposited particles begins to form on top of the support walls. This is exactly what happens when the deposition takes place with a slurry of particles with dimensions of the order of few microns (Fig. 1b).

As it has already been mentioned,[17] at low solids concentrations in the sol, filtration starts with pore clogging: the support becomes saturated with the sol very fast and the capillary pressure drop disappears before cake filtration can take place. The result is the absence of a surface layer. The sol that is entrapped in the pores converts to a gel during the subsequent drying stage. This is the situation described in Fig. 1a. At higher solids concentrations, filtration starts immediately and a surface layer ("cake") begins to form by a mechanism similar to that used in slip-casting. When the concentration of solids

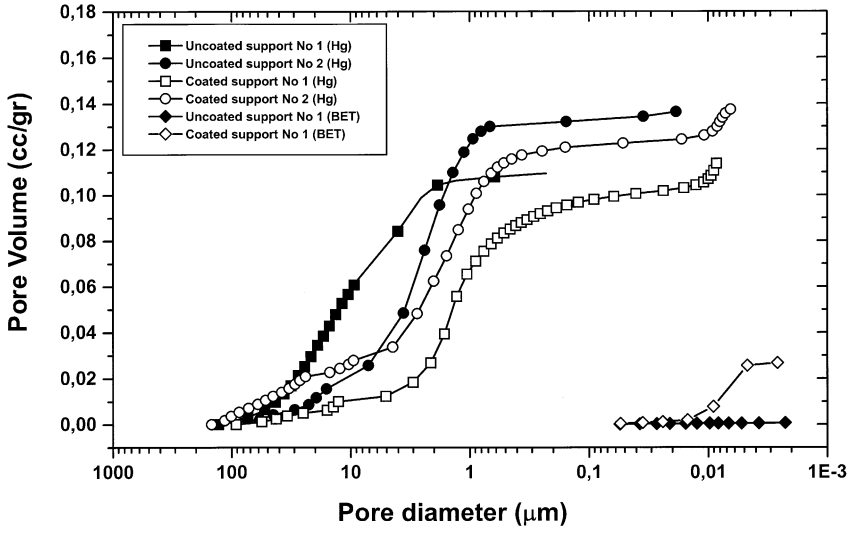

Fig. 7. Pore size distributions of the un-coated and coated cordierite substrates.

in the cake exceeds a critical value, the sol is converted to a gel. Progressively the gel layer builds up and its filtration resistance increases; when this resistance exceeds a critical value, the process stops. The slip-casting model predicts that the thickness of the membrane increases with the square root of time and is inversely proportional to the square root of the viscosity of the coating sol.[17]

However, when the coating is taking place with a highly viscous sol there is a second contribution to the formation of the coating layer due to viscous forces. As the support is withdrawn from the sol a part of the sol is adhered as a thin film on the support walls (by a mechanism similar to that used in dip-coating processes). A part of the total gel layer thickness results from this adhered sol layer[17] which becomes progressively concentrated in solid particles due to evaporation during drying. It is obvious that the thickness of this adhered layer increases with sol viscosity and in fact, from the theory of dip coating occurs that the coating thickness is proportional to the square root of the sol viscosity and of the withdrawal speed.[5]

For a porous support, if the sol viscosity is sufficiently low, this adhered layer is negligible and the loading percentage (and consequently the coating layer thickness) is dictated by the capillary filtration that takes place on the channel surface. The main resistance to filtration is due to the low permeability of the deposited nanophase coating layer, since on one hand, sol viscosity is low and on the other hand the support mean pore size is large enough so that the filtration resistance of the support is negligible. Therefore, the effects of differences in the support mean pore size or the sol viscosity cannot be distinguished. Because of the very small size of the particles deposited and the consequent very tight packing (Fig. 6), the filtration resistance of the coating layer becomes large, even when this layer is thin; therefore, the filtration process stops at small coating thickness.

On the other hand, as the sol viscosity increases, the percentage of the adhered layer also increases; the coating thickness contributed by the capillary filtration is, in this case, much less compared to that contributed by the adhered film due to viscous forces. Thus, for a given support, the coating thickness is dictated primarily by the adhered part of the coating and, therefore, increases with increasing viscosity. This is the case described by the plots in Figs. 3 and 4. Similar results were obtained by Cini et al.[14] who observed that in the preparation of γ-alumina membranes from boehmite sols upon tubular α-alumina supports with mean pore diameter of 3 μm, thicker membranes were produced from the sols of higher viscosities.

To explain the difference in loading percentage at high viscosities for the two porous supports observed in Fig. 3, it is reasonable to assume that a certain amount of the viscous sol fills the surface pores of the support before surface filtration starts. This amount of solids trapped in the surface pores is higher in the case of the support with the larger pores and can be considered responsible for the difference in weight between the two kinds of coated supports. This surface pores filling probably helps in better anchoring the membrane layer on the support; however, the penetration depth is limited very close to the outer channel surface and the degree of penetration is not at all comparable to that depicted in Fig. 1.

The pore size distributions of the coated and the uncoated supports were studied with the aid of both nitrogen and mercury porosimetry. The results are summarized in

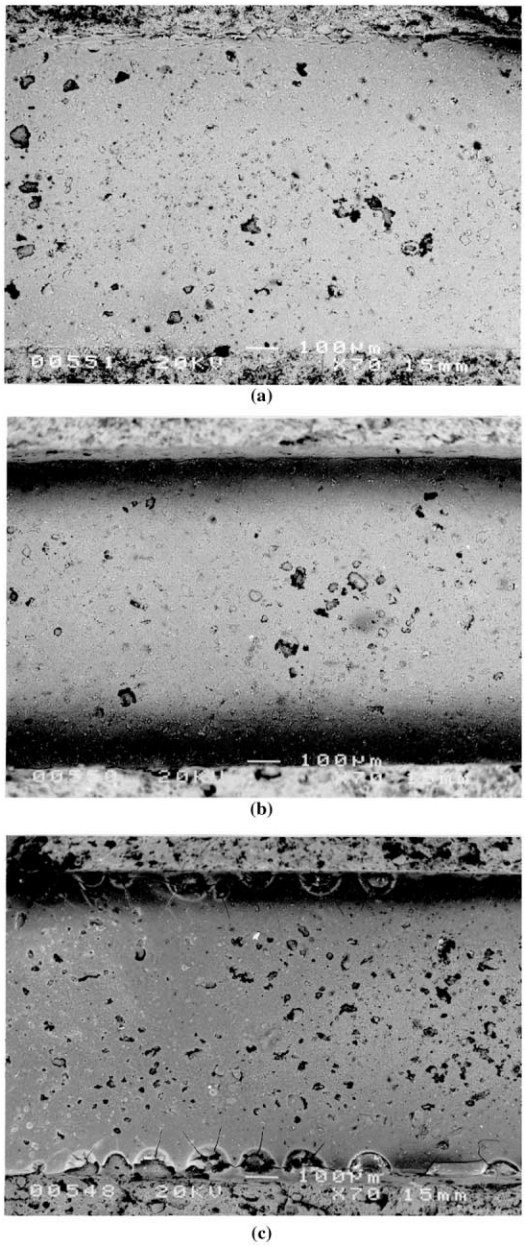

Fig. 8. Effect of sol viscosity on the quality of the deposited coating. Scanning electron microscopy photographs (top-view) of the covered honeycomb channels for the same cases as in Fig. 5 (honeycomb with mean pore size $d_p = 10$ μm, coated with a sol containing 20 wt.% binder: (a) no sol concentration; (b) concentration of the sol to 55% of its initial weight; (c) concentration of the sol to 40 wt.% of its initial weight.

Fig. 7. As far as the uncoated supports are concerned, the difference in their mean pore size is obvious from the relevant mercury porosimetry data, whereas the respective nitrogen porosimetry curve (right lower corner) for the support with $d_{p50} = 10$ μm, reveals the total absence of meso- and micro-porosity. (The situation is the same for the uncoated support with $d_{p50} = 3$ μm; this is the reason why the relevant nitrogen porosimetry curve is not shown in Fig. 7).

The mercury porosimetry curves for the coated supports (Fig. 7) show the combined influence of the support and of the coating layer. On one hand the presence of the coating is indicated by the step of the curve observed at the lower end of the mercury porosimetry curves (0.01 μm — meso-porosity region). A clearer picture is obtained from the respective nitrogen porosimetry curves shown at the right lower corner of Fig. 7. The nitrogen porosimetry data for the coated support indicate a mean pore diameter of 7.0 nm, corresponding to the pore size of the deposited coating. This mean pore size is three orders of magnitude less than the respective pore diameter of the support. On the other hand, the presence of the coating shifts the apparent mean pore size of the support obtained from mercury porosimetry, towards smaller values. Indeed, the first inflection points of the curves for the two coated supports, correspond to mean pore sizes of 1.5 and 2 μm, compared to $d_{p50} = 10$ and 3 μm, respectively, for the same un-coated supports. This trend is always observed on such systems.[25] Because of the presence of the "tight" coating around the support walls, a higher pressure is required for the penetration of mercury in the support; this has, as a result, the appearance of a mean support pore diameter much less than the actual one. In reality, the coated support No. 1 for instance, does not have the pore size distribution described by the respective curve in Fig. 7, but possesses a support mean diameter of 10 μm, coated with a layer with mean pore size of 7.0 nm.

The surface area of a support No. 2 (i.e. with the mean pore diameter of 10 μm), coated with 7.9 wt.% of γ-alumina was measured at 11.3 m^2/g, compared to the negligible specific surface area (0. 02 m^2/g) of the uncoated support. The respective surface area of the γ-alumina powder that occurred from the calcination of boehmite at 600°C for 2 h was 173.2 m^2/g; thus the specific surface area of the whole pellet corresponds well to the relevant loading percentage value.

However, as the loading percentage, and consequently the coating thickness increases, the integrity of the coating cannot be equally well maintained; cracks are beginning to appear (Fig. 5c). A comparison of coating integrity for the three cases above, is presented in Fig. 8 where the top view of a single coated monolith channel is shown under the same magnification. For the thickest coating, the appearance of large cracks, concentrated close to the channel edges is evident. The increase in

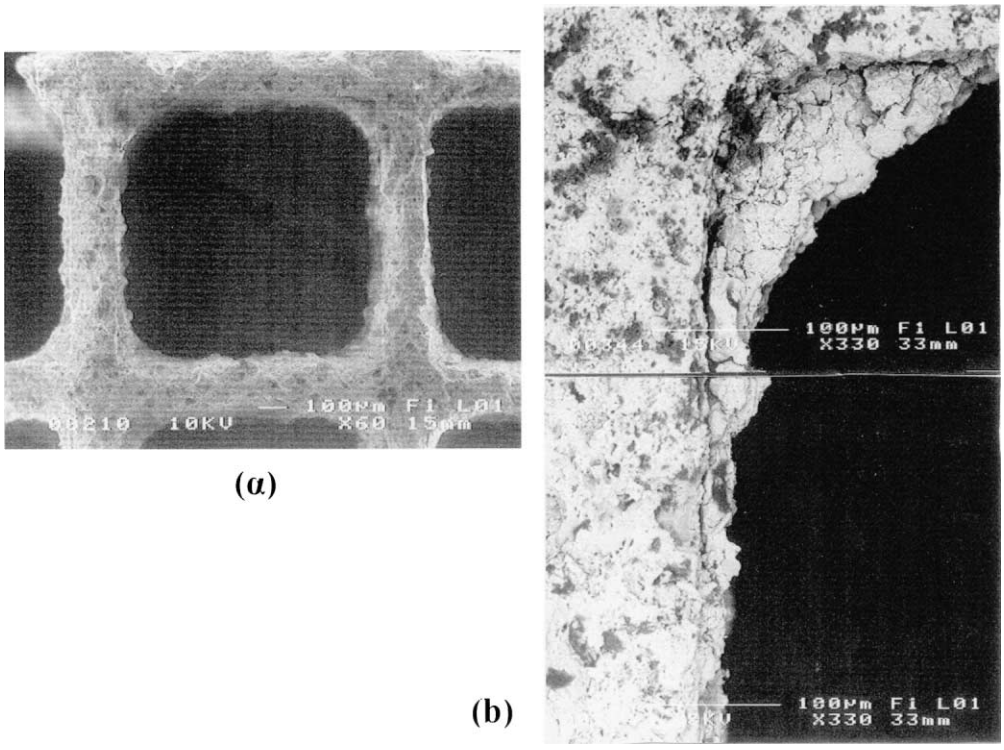

Fig. 9. Coating with a sol/powder coating medium: (a) coating thickness and uniformity in the honeycomb channels; (b) magnification of a coated wall so that the morphology of the coating can be directly compared to that obtained from a sol of very low viscosity (Fig. 1a) and to that obtained from a powder slurry (Fig. 1b).

coating thickness produces a higher shrinkage gradient that induces higher stresses during drying, which in turn initiate crack formation. It is clear that there exists an optimum value of coating thickness, which during drying can lead to crack-free coatings. However, a film that is too thin, may not cover completely all the mouths of the largest pores resulting thus in, the so-called pinhole defects, which are crucial for the performance of a gas separation membrane. Such pinholes are evident in all three cases presented in Fig. 8. As Cini et al.[13] have remarked, there exists a trade-off between thick films that develop cracks and thin films that induce pinholes. Repeated dipping has been suggested by Terpstra et al.[26] as an effective way to cure this pinhole defect and has been widely applied in the membrane preparation literature.[27]

Extensive cracks can be detrimental to the coating integrity, and on the adhesion of the coating on the support; on the other hand repeated impregnations and subsequent calcinations are lengthy and costly. In order to combine the high loading percentage and the formation of a surface coating achieved with powder slurries with the high activity, surface area and ease of mixing obtained with sols, we used a "hybrid" system as coating medium: a sol of the same boehmite powder used above, but to which we have added a significant amount of $Al(OH)_3$ commercial powder.[d] By adjusting the pH to 4.0 with the addition of HNO_3, a slurry with 50 wt.% solids loading could be obtained with viscosity of only 63 mPa s^{-1}. The characteristics of the slurry and the loading achieved are also summarized in Table 1. The slurry viscosity could be further fine-tuned by adjusting the proportions of boehmite/$Al(OH)_3$ powders — no binders were necessary in this case. Because of the higher slurry solids content, loadings achieved with this coating medium were between 12.5 and 13.5 wt.% per impregnation, significantly higher than those obtained from the boehmite sols (2–8 wt.% depending on sol viscosity). Honeycombs with characteristic mean pore diameter 10 μm, coated with this medium are shown in Figs. 9–11 in progressively higher magnifications. In Fig.9a, the thickness of the coating, indicative of the high loading percentage, and the coating uniformity from channel to channel can be clearly observed. A coated wall upon which a surface coating has been deposited is shown in Fig. 9b, at a magnification similar to that of Fig.1a. It can be very clearly seen that the morphology of the coating deposited with the sol/slurry system is something "in-between" the ones shown in Figs 1a and b. A much clearer view can be grasped from Fig. 10a where the wall/coating interface is shown and from Fig. 10b, where the details of the coating microstructure can be distinguished. It is clear from Fig. 10a, that the interaction between the $Al(OH)_3$ powder particles and the colloidal boehmite particles in the coating medium prevents the latter from penetrating into the wall pores: a surface coating is formed where gel-like regions are "binding" the powder particles together.

Not only the loading percentages achieved with this hybrid sol/powder system were high, but the photographs of the wall/coating interface indicate excellent adhesion: the gel-like coating layer seems to be firmly attached on the support walls with no visible gaps. In previous works[28,29] we have measured the adhesion of coatings deposited from powder slurries and we have shown that the characteristic powder diameter has to be reduced to the order of 2–6 μm, in order to achieve adhesion comparable to that of a commercial catalyst system. Indeed, adhesion measurements with the apparatus previously reported[28,29] have shown (Fig. 11) that the sol/slurry hybrid coating exhibited superior adhesion than coatings obtained with slurries of finely ground particles as well as from a commercial catalyst system. The thermal stability of these supports (effects of precursor materials, additives and operating temperature on phase development, pore structure and surface area reduction) will be the subject of another publication.

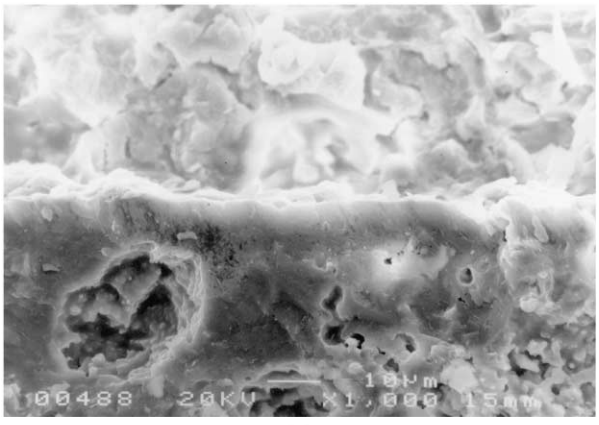

(a)

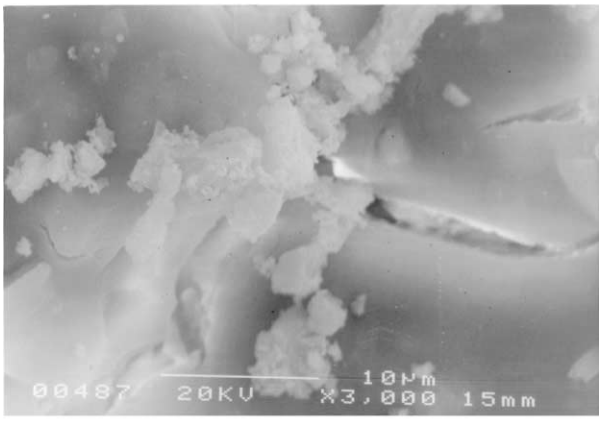

(b)

Fig. 10. Coating with a sol/powder coating medium: (a) magnification of the support/coating interface; (b) detail of the coating microstructure.

[d] Merck GmbH, Darmstad, Germany.

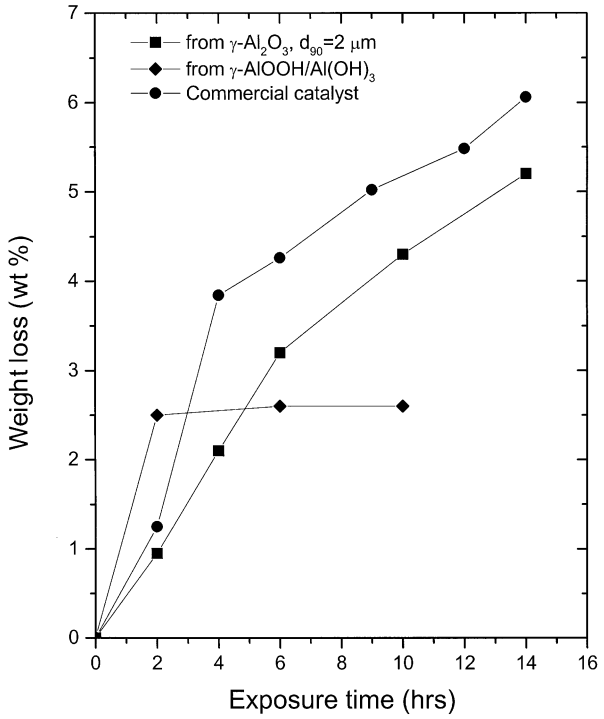

Fig. 11. Adhesion performance (weight loss as a function of the exposure time in a hot gas stream) of coatings obtained from the various routes tested.

Porous ceramic supports are constantly gaining ground in hot gas treatment; materials other than cordierite are tested as supports[30] and their characteristics are adapted and tailor-made to the particular application. On one hand honeycombs with much "denser" structure (1000 cells/in^{-2}) are within the manufacturing priorities of the car exhaust manufacturers, whereas on the other hand, supports with a much more "open" structure such as ceramic foams, are employed in catalytic combustion.[31,32] The matching of the rheological properties of the coating medium to the characteristics of the porous structure of the support is therefore imperative for the achievement of a successful and operational support/coating system. Currently, we run experiments for the preparation of supports with mean pore sizes and porosities within a much wider range, not only from cordierite, but from other materials with high thermal shock resistance, so that guidelines for the optimum combination of support pore structure and sol rheological properties for the deposition of multilayered, thick, crack-free coatings can be established.

4. Conclusions

Even though sol-gel methods are inherently appropriate for the preparation of meso-porous coatings with tailor-made properties such as catalyst carriers or membranes, there exist technological problems when the particular application requires a macro-porous support such as the honeycombs used in high temperature heterogeneous catalysis systems.

Sols of colloidal boehmite can be used for the deposition of meso-porous coatings upon honeycombs, provided that their viscosity is adjusted with the addition of viscous binders and sol concentration. The loading percentage and the thickness of the deposited coating increase with sol viscosity. There exists, however, an upper coating thickness limit (about 5 μm in the particular case under study), beyond which significant crack development occurs that can deteriorate the adhesion of a catalyst support and is certainly detrimental on the performance of a separation membrane.

The combination of finely ground powders (with characteristic diameters 2–5 μm) with colloidal ones in the coating medium can limit the sol infiltration into the support pores. Such a coating medium also provides for higher loading per impregnation and deposition of thicker coatings with better adhesion on the support.

References

1. Heck, R. M. and Farrauto, R. J., *Catalytic Air Pollution Control-Commercial Technology*. Van Rostrand Reinhold, New York, 1995.
2. Geus, J. W. and van Giezen, J. C., Monoliths in catalytic oxidation. *Catal. Today,* 1999, **47**, 169–180.
3. Schneider, R., Kiessling, D. and Wendt, G., Cordierite monolith supported perovskite-type oxides — catalysts for the total oxidation of chlorinated hydrocarbons. *Appl. Catal. B,* 2000, **28**, 187–195.
4. Murrell, L. L., Sols and mixtures of sols as precursors of unique oxides. *Catal. Today,* 1997, **35**, 225–245.
5. Hsieh, H. P., *Inorganic Membranes for Separation and Reaction*. Elsevier Science, Amsterdam, 1996.
6. Guizard, C., Julbe, A., Larbot, A. and Cot, L., Ceramic membrane processing. In *Chemical Processing of Ceramics*, ed. E. J. A. Pope and B. I. Lee. Marcel Dekker, New York, 1994, pp. 501–531.
7. Guizard, C., Julbe, A., Ayral, A., Ramsay, J. and Larbot, A., Recent advances in ceramic membrane processing. In *Ceramics: Charting the Future*, ed. P. Vincenzini. Techna Srl, 1995, pp. 2743–2754.
8. Guizard, C., Mouchet, C., Vacassy, R., Julbe, A. and Larbot, A., Sol-gel processing of inorganic membranes. *J. Sol-Gel Sci. Technol.,* 1994, **2**, 483–487.
9. Yeung, K. L., Sebastian, J. M. and Varma, A., Mesoporous alumina membranes: synthesis, characterization, thermal stability and non-uniform distribution of catalyst. *J. Memb. Sci.,* 1997, **131**, 9–28.
10. Lafarga, D., Lafuente, A., Menendez, M. and Santamaria, J., Thermal stability of γ-Al_2O_3/α-Al_2O_3 mesoporous membranes. *J. Memb. Sci.,* 1998, **147**, 173–185.
11. Ekonomakou, A., Tsetsekou, A. and Stournaras, C. J., An investigation of the processing parameters for cordierite honeycombs production. In *Ceramics: Charting the Future*, ed. P. Vincenzini. Techna Srl, 1995, pp. 2439–2448.
12. Saracco, G. and Montanaro, L., Catalytic ceramic filters for fluegas cleaning. 1. Preparation and characterization. *Ind. Eng. Chem. Res.,* 1995, **34**, 1471–1479.
13. Cini, P., Blaha, S. R., Harold, M. P. and Venkataraman, V., Preparation and characterization of modified tubular ceramic mem-

branes for use as catalyst supports. *J. Membr. Sci.,* 1991, **55**, 199–225.
14. Cini, P. and Harold, M. P., An experimental study of the tubular supported ceramic membrane as a multiphase catalyst. *AIChE J.,* 1991, **37**, 997–1008.
15. Santos, L. R. B., Pulcinelli, S. H. and Santilli, C. V., Formation of SnO_2 supported porous membranes. *J. Sol-Gel Sci. Technol.,* 1997, **8**, 477–481.
16. Leenaars, A. F. M., Keizer, K. and Burggraaf, A. J., The preparation and characterization of alumina membranes with ultra-fine pores, Part 1. Microstructural investigations on non-supported membranes. *J. Mater. Sci.,* 1984, **19**, 1077–1088.
17. Leenaars, A. F. M. and Burggraaf, A. J., The preparation and characterization of alumina membranes with ultra-fine pores, Part 2. The Formation of supported membranes. *J. Colloid Interface Sci.,* 1985, **105**(1), 27–40.
18. Burggraaf, A. J., Keizer, K. and vanHassel, V. A., Ceramic nanostructure materials, membranes and composite layers. *Solid State Ionics.,* 1989, **32/22**, 771–782.
19. Ulhorn, R., Huis In't Veld, M. H. B. J., Keizer, K. and Burggraaf, A. J., Synthesis of ceramic membranes, Part I: synthesis of non-supported and supported γ-alumina membranes without defects. *J. Mater. Sci.,* 1992, **27**, 527–537.
20. Zaspalis, V. T., Van Praag, W., Keizer, K., Ross, J. R. H. and Burggraaf, A. J., Synthesis and characterization of primary alumina, titania and binary membranes. *J. Mater Sci.,* 1992, **27**, 1023–1035.
21. Lin, Y. S., deVries, K. J. and Burggraaf, A. J., Thermal stability and its improvement of the alumina membrane top-layers prepared by sol-gel methods. *J. Mater. Sci.,* 1991, **26**, 715–720.
22. Lin, Y., Chang, C. and Gopalan, R., Improvement of thermal stability of porous nanostructured ceramic membranes. *Ind. Eng. Chem. Res.,* 1994, **33**, 860–870.
23. Luyten, J., Cooymans, J., Smolders, C., Vercauteren, S., Vansant, E. F. and Leysen, R., Shaping of multi-layer ceramic membranes by dip coating. *J. Eur. Ceram. Soc.,* 1997, **17**, 273–279.
24. Lindqvist, K. and Liden, E., Preparation of alumina membranes by tape casting and dip coating. *J. Eur. Ceram. Soc.,* 1997, **17**, 359–366.
25. Hayes, R. E., Kolaczkowski, S. T., Li, P. K. C. and Awdry, S., Evaluating the effective diffusivity of methane in the washcoat of a honeycomb monolith. *Appl. Catal. B.,* 2000, **25**, 93–104.
26. Terpstra, R. A., Bonekamp, B. C., vanVeen, H. M., Engel, A. J. G., deRooy, R. and Veringa, H. J., Preparation and properties of tubular ceramic Al_2O_3 membranes for gas separation. In *Science of Ceramics 14*, ed. D. Taylor. 1988, pp. 557–566.
27. Kim, J. and Lin, Y. S., Synthesis and characterization of suspension-derived porous ion-conducting ceramic membranes. *J. Am. Ceram. Soc.,* 1999, **82**(10), 2641–2646.
28. Agrafiotis, C., Tsetsekou, A. and Ekonomakou, A., The effect of particle size on the adhesion properties of oxide washcoats on cordierite honeycombs. *J. Mater. Sci. Lett.,* 1999, **18**, 1421–1424.
29. Agrafiotis, C. and Tsetsekou, A., The effect of powder characteristics on washcoat quality: Part I. Alumina washcoats. *J. Eur. Ceram. Soc.,* 2000, **20**, 815–824.
30. Inoue, H., Sekizawa, K., Eguchi, K and Arai, H., Thick-film coating of hexaaluminate catalyst on ceramic substrates for high-temperature combustion. *Catal. Today,* 1999, **47**, 181–190.
31. Richardson, J. T., Peng, Y. and Remue, D., Properties of ceramic foam catalyst supports: pressure drop. *Appl. Catal. A,* 2000, **204**, 19–32.
32. Van Setten, B. A. A. L., Bremmer, J., Jelles, S. J., Makkee, M. and Moulijn, J. A., Ceramic foam as a potential molten salt oxidation catalyst support in the removal of soot from diesel exhaust gas. *Catal. Today,* 1999, **53**, 613–621.